



Contents lists available at ScienceDirect

Journal of Pharmaceutical Sciences

journal homepage: www.jpharmsci.org

Pharmaceutical Nanotechnology

Highly Water-Soluble Orotic Acid Nanocrystals Produced by High-Energy Milling

Jéssica de Cássia Zaghi Compri¹, Veni Maria Andres Felli¹, Felipe Rebello Lourenço¹, Takayuki Takatsuka², Nikoletta Fotaki³, Raimar Löbenberg⁴, Nádia Araci Bou-Chacra^{1,*}, Gabriel Lima Barros de Araujo¹

¹ Department of Pharmacy, Faculty of Pharmaceutical Sciences, University of São Paulo, São Paulo, Brazil

² Thinky Corporation, Tokyo, Japan

³ Department of Pharmacy & Pharmacology, University of Bath, Bath, UK

⁴ Faculty of Pharmacy and Pharmaceutical Sciences, University of Alberta, Edmonton, Canada

ARTICLE INFO

Article history:

Received 5 July 2018

Revised 18 December 2018

Accepted 20 December 2018

Keywords:

nanotechnology

nanocrystal(s)

physical characterization

physicochemical

solubility

formulation

stability

polymer(s)

surfactant(s)

stabilization

ABSTRACT

Orotic acid (OA), a heterocyclic compound also known as vitamin B13, has shown potent antimalarial and cardiac protection activities; however, its limited water solubility has posed a barrier to its use in therapeutic approaches. Aiming to overcome this drawback, OA freeze-dried nanocrystal formulations (FA, FB, and FC) were developed by using the high-energy milling method. Polysorbate 80 (FA) and povacoat[®] (FC) were used alone and combined (FB) as stabilizers. Nanocrystals were fully characterized by dynamic light scattering, laser diffraction, transmission electron microscopy, thermal analysis (thermogravimetry and derivative thermogravimetry, and differential scanning calorimetry), and X-ray powder diffraction revealing an acceptable polydispersity index, changes in the crystalline state with hydrate formation and z-average of 100–200 nm, a remarkable 200-time reduction compared to the OA raw material (44.3 μm). Furthermore, saturation solubility study showed an improvement of 13 times higher than the micronized powder. In addition, cytotoxicity assay revealed mild toxicity for the FB and FC formulations prepared with povacoat[®]. OA nanocrystal platform can deliver innovative products allowing untapped the versatile potential of this drug substance candidate.

© 2019 American Pharmacists Association[®]. Published by Elsevier Inc. All rights reserved.

Introduction

Orotic acid (OA) is a heterocyclic compound, whose structure, functions, and potential pharmacologic actions have been studied for many years. This compound, also named vitamin B13, is produced by the human intestinal flora and it is found in many biological processes. It actively participates in the urea cycle and it is one of the precursors in pathway synthesis *de novo* of pyrimidines for replication of DNA and RNA.^{1,2}

One of the most relevant pharmacological findings is its anti-malarial action. OA derivatives can inhibit the activity of 2 key enzymes in Plasmodium replication within the host: dihydroorotase and dihydroorotate dehydrogenase³ showing a desirable selective toxicity. The parasite dies from pyrimidine deficiency, while

the patient is able to maintain their pyrimidine synthesis of uridine and cytidine nucleotides.⁴

Furthermore, studies in animals have shown that OA can provide cardiac protection, contributing to the prevention of myocardium degeneracy and heart failure in animals with genetic cardiomyopathies.⁵ Additionally, some researchers revealed the use of OA as a food supplement for high-performance athletes. Its effects occur during physical activities by improving and maintaining adenosine triphosphate levels in glucose uptake. This increases the formation of ribose and muscle carnosine storage, supporting and strengthening muscle hypertrophy and increasing the contractile capacity of muscle.^{6–8} In the cosmetic area, it presents a moisturizing effect on skin, with an effect comparable to excipients with highly moisturizing properties, such as the pyrrolidone carboxylic acid.

Although OA presents potential therapeutic properties, its aromatic nature, characterized by the presence of a pyrimidine ring, confers low water solubility to the molecule in the physiological pH range.⁹ Aiming to overcome this limitation, the development of OA

* Correspondence to: Nádia Araci Bou-Chacra (Telephone: 551130913628).

E-mail address: chacra@usp.br (N.A. Bou-Chacra).

synthetic derivatives with improved solubility has been explored as an alternative approach. These modifications take advantage of its multidentate structure by adding substituents in its pyrimidine ring, in the heterocyclic nitrogen atoms in the carboxylic oxygens, as well as in the carboxylic group.¹⁰ However, the efficacy of these compounds remains unknown.

Recent advances in drug delivery systems can overcome this solubility problem, while maintaining the drug safety profile, such as the use of nanotechnologies. Among these, nanocrystal drugs are one of the most effective approaches.^{11,12} Nanocrystals are defined as nanometer-sized particles produced from pure drugs, which are usually stabilized by surfactants and/or polymeric steric stabilizers present in the dispersion medium. In addition, they are obtained in a liquid dispersion, called nanosuspension.¹³⁻¹⁵ They have been present in the pharmaceutical market since the 2000s, when Rapamune® (immunosuppressant) was launched. Ever since, they have been one of the most promising nanostructures, due to their high earnings and low time-to-market character. By 2017, the Food and Drug Administration has received more than 80 applications for nanocrystal drug products.¹⁶ Nowadays nanocrystals comprise a list of at least 17 products on market such as Emend® (prevention of chemotherapy-induced nausea and vomiting), Tricor® (cholesterol-lowering drug), Triglide® (lipid regulation), Avinza® (phychoestimulant), Ritalin LA® (central nervous system stimulant), Zanaflex® (muscle relaxant), Megace® (improvement of appetite and increase in body weight in patients with cancer-associated anorexia), and Naprelan® (anti-inflammatory).^{11,13,17,18} To the best of our knowledge, there is no OA nanocrystal reported in the literature.^{15,19}

Different technologies were developed to obtain nanocrystals. In general, the processes are classified into 2 categories, top-down and bottom-up.^{20,21} Among these technologies, high-energy milling, a top-down method, is impressive due to several advantages, such as the short time required in the process and the simplicity in development and in the scaled-up production.²²⁻²⁴ Despite these numerous advantages, the additional free energy of the new surfaces generated by the milling needs to be compensated to avoid instability, which can be achieved by the use of proper stabilizers.¹⁹⁻²¹ As the selection of stabilizers is often drug specific, the search for new and more efficient stabilization systems is needed.^{25,26} Recently, povacoat®, a polyvinyl alcohol copolymer derivative, has been pointed out as a promising new stabilizer for nanocrystal formulations.^{27,28} In the present study, we report the beneficial effects of the use of this copolymer and a new combination with polysorbate 80, one of the most popular stabilizers, for the development and cytotoxicity evaluation of OA nanocrystals.

Experimental Section

Materials

OA anhydrous (purity 99.8%) (Fig. 1) was purchased from Sigma Aldrich (São Paulo, Brazil). Methylcellulose, polysorbate 80, methylparaben, and glucose were obtained from Shin-Etsu (Tokyo,

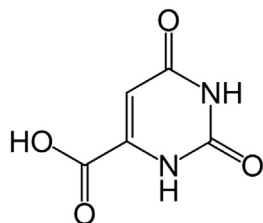


Figure 1. Molecular structure of orotic acid.

Japan). Povacoat® type F (polyvinyl alcohol/acrylic acid/methyl methacrylate copolymer) was donated from Daido Chemical Corporation (Osaka, Japan). Hydrochloric acid, sodium chloride, sodium citrate, sodium acetate, potassium phosphate monobasic, and sodium hydroxide were obtained from Synth (Sao Paulo, Brazil). Purified water was obtained from a Milli-Q Millipore water system (São Paulo, Brazil). The cell line NCTC clone 929 was donated from the Culture Section of the Cell Institute Adolfo Lutz (São Paulo, Brazil). The culture media was purchased from Interlab (São Paulo, Brazil).

Methods

Preparation of OA Nanocrystals

OA nanocrystals were prepared using a rotation revolution nanopulverizer NP-100 (Tokyo, Japan) according to the method proposed by Takatsuka et al.²² Before the nanopulverization, a dispersion medium was prepared by dissolving the following stabilizers: methylcellulose (0.3% w/v), povacoat® (10% w/v), and polysorbate 80 (0.1% w/v) in the water. Three formulations were prepared using polysorbate 80 (FA), polysorbate 80 and povacoat® together (FB), and povacoat® (FC). The concentration of the OA was maintained constant at 10% (w/v).

The nanopulverization was performed in 2 steps. In the first step, 10 g of OA and 50 g of the aqueous solution containing the stabilizers were transferred to the mixing vessel. A total of 35 g of yttrium-stabilized zirconia milling beads with a diameter of 0.1 mm were added to the same container. At this stage, the conditions for pulverization were 1500 rpm for 15 min. For the second step, 50 g of aqueous solution containing the stabilizers were added to the vessel and the conditions applied were 400 rpm for 1 min.

From the nanosuspensions obtained, an amount of 10 g was immediately freeze-dried (Christ Alpha 1-5, Christ Martin, Germany) at -70°C for 48 h under pressure of 0.120 mbar and 24°C using glucose (up to 5 g) to prevent aggregation.

Characterization of OA Nanocrystals

Process Efficacy and Influence of the Stabilizer on Particle Size, Zeta Potential, and Stability

OA particle size distribution was measured using laser diffraction technique (Mastersizer 2000; Malvern Instruments, Malvern, UK) with a small volume dispersing unit (Hydro 2000uP; Malvern Instruments). Samples were diluted 20-fold using Ultrapure Milli-Q® water. The nanocrystals z-average was measured by dynamic light scattering (DLS) technique using a Zetasizer Nano ZS device (Malvern Instruments). The samples were diluted in Milli-Q® in the ratio of 1:400 (nanocrystal:water). Measurements were performed in triplicate using a measurement angle of 90° .

The zeta potential (ZP) was determined employing a Zetasizer Nano ZS 90 device (Malvern Instruments). Samples ($n = 3$) were prepared using 20 μL of a diluted nanosuspension in 4 mL of Milli-Q® water. The conductivity of the dispersion was adjusted to 50 $\mu\text{S}/\text{cm}$, with NaCl solution at pH 5.5.²⁹

The stability of the freeze-dried nanosuspensions, kept under refrigeration (4°C), was evaluated by monitoring the variations in particle size distribution and z-average, polydispersity index (PDI), and ZP values, for 3 months. Data were analyzed using Minitab 17 Statistical Software® by analysis of variance (ANOVA) and regression analysis. p values less than 0.05 were considered statistically significant. Additionally, macroscopic observations aiming to detect sediment and agglomerates in the redispersed nanosuspensions were performed monthly.

Scanning Electron Microscopy

OA raw material was analyzed using an SU-1500 scanning electron microscope (SEM) (Hitachi High-Technologies, Tokyo, Japan). Samples were measured using 15 kV acceleration voltage and images were acquired using 500 \times magnification. The morphology and particle size of nanocrystals were observed using a transmission electron microscopy JEM-1010 with 80 kV (Jeol USA). Samples were obtained from a saturated solution and diluted 10 \times . The material was deposited on copper grids and coated with 150 Mesh Formvar film for 10 min. In addition, Image J[®] Software was used for the crystal size confirmation. The analysis was performed individually for OA raw material, FA, FB, and FC, for which 30 crystals were measured per sample ($n = 30$).

Thermal Analysis

Differential scanning calorimetry (DSC) curves were obtained in a DSC 7020 (Exstar, Tokyo, Japan). About 2 mg of samples (pure materials, physical mixture, and nanocrystals) was placed in an aluminum sample holder hermetically sealed and subjected to analysis. Dynamic N₂ atmosphere (50 mL min⁻¹) and a heating rate of 5°C min⁻¹ in the temperature range of 25°C-300°C were used. The temperature range and enthalpy response were previously calibrated using an indium standard.

Thermogravimetry and derivative thermogravimetry (TG/DTG) curves were obtained using a TG/DTA 7200 (Exstar), with sample weight of approximately 5 mg (platinum crucible) at a heating rate of 5°C min⁻¹, under dynamic N₂ atmosphere (100 mL min⁻¹) in the temperature range 25°C-600°C. The instrument calibration was verified employing calcium oxalate standard.

X-Ray Diffraction

A Bruker Diffractometer Model D8 Advance Da Vinci (Bruker, Yokohama, Japan) was used to characterize the solid crystalline state. Samples of the physical mixture in absolute values and nanocrystals were exposed to Cu K α radiation 40 Kv. Measurements were performed at a scanning speed of 0.5°/min over a 2 θ range of 0.01°-40°.

Determination of Saturation Solubility

The saturation solubility of FA, FB, and FC was determined by shake-flask method.³⁰ The media were determined in an exploratory experiment where OA showed more solubility in media acetate pH 4.5 and water. The formulations were added to vials containing 10 mL media. After reaching saturation, the vials were properly sealed and transferred to a shaker, 430-RDBPE model (New Ethics, São Paulo, Brazil) at 37°C for 72 h. At the end of that period, aliquots were collected and filtered using a porous micron full-flow 45- μ m filter (Millex GM, Millipore, MA), and the solubilized amount of OA was determined by spectrophotometric method.

Determination of OA Content

OA content in the nanosuspension was determined by UV spectrophotometry using an Evolution[™] 201 UV-Visible Spectrophotometers (Thermo Scientific, São Paulo, Brazil) and wavelength of 274 nm. The method was developed and validated in the parameters of specificity, linearity, accuracy, and precision.

Cytotoxicity

Cell line NCTC clone 929 (mouse connective tissue) CCIAL020, grown in minimal medium Eagle supplemented with 0.1 mM nonessential amino acids, 1.0 mM sodium pyruvate, and 10% fetal bovine serum without antibiotic was used in the agar diffusion method.^{31,32} Samples were tested in 4 replicates on separate plates; for the positive controls, latex fragments (toxic) were used (0.5 cm \times 0.5 cm); and negative controls were filter paper discs,

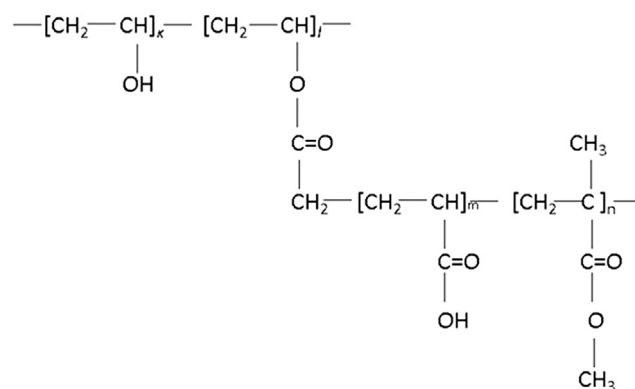


Figure 2. The chemical structure of water-soluble polymer povacoat[®] type F.

respecting the dimensions of 0.5 cm in diameter. Samples were analyzed macroscopically observing the presence or absence of a clear halo in or around the test sample. The diameters of these halos, when present, were accurately measured, using a calibrated

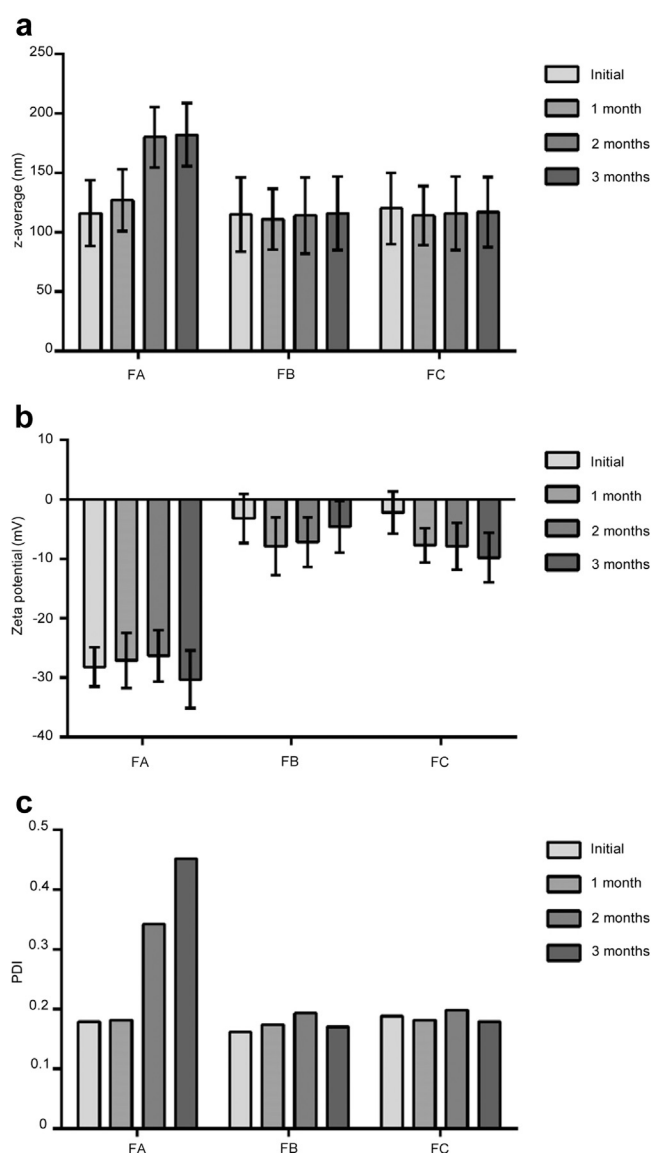


Figure 3. (a) Z-average, (b) zeta potential, and (c) polydispersity index of FA, FB, and FC for 3 months.

pachymeter. The average of the readings of halo diameters of 4 plates was calculated.

Results and Discussion

Process Efficacy and Influence of the Stabilizer on Particle Size, ZP, and Stability

The z-average, the PDI, and ZP of FA, FB, and FC were obtained immediately after preparation. The mean particle size values of nanocrystals were 116 ± 5 nm (FA), 115 ± 6 nm (FB), and 120 ± 6 nm (FC). PDI was 0.170, 0.162, and 0.188 and the ZP was -28.2 ± 5.7 mV, -3.2 ± 7.2 mV, and -2.2 ± 6.1 mV, respectively, for FA, FB, and FC. The weight mean volume D[4.3] of the OA raw material determined by laser diffraction was $26.1 \mu\text{m}$. The surface-weighted mean D[3.2] was $18.5 \mu\text{m}$ and the PDI value was 0.424. Additionally, the diameter at 10%, 50%, and 90% of the cumulative population distribution were $d_{0.1} = 11.7 \mu\text{m}$, $d_{0.5} = 23.9 \mu\text{m}$, and $d_{0.9} = 44.3 \mu\text{m}$. Comparing with FA, FB, and FC, the reduction in particle size was more than 200 times in all formulations (raw material $d_{0.5} = 23.9 \mu\text{m}$; [FA] 116 ± 5 nm, [FB] 115 ± 6 nm, and [FC] 120 ± 6 nm). These results indicate a highly effective performance of the high-energy milling method of producing OA nanocrystals. As examples for comparisons, Takatsuka et al.²² prepared nanocrystals of 5 poorly water-soluble compounds (Biopharmaceutics Classification System class II and IV) by high-energy milling. The most notable reduction was obtained for nifedipine with the particle size reduction of $d_{0.5}$ in 105 times ($d_{0.5} = 14.6$ mm to 139 nm). Similarly, Barbosa et al.¹⁷ obtained furosemide nanocrystals by the same method reducing the $d_{0.5}$ about 29 times from particles of $3.6 \mu\text{m}$ down to $d_{0.5}$ of 122 nm.

The stability study was performed using the dry formulation storage in glass vessel at 4°C . The z-average, PDI, and ZP values obtained during the 3 months in the stability test are presented in Figure 1. After 3 months, the values obtained were 182 ± 5 nm, 116 ± 5 nm, and 117 ± 4 nm, demonstrating that only the formulation without povacoat[®] (FA) presented an increase in z-average over the period of 3 months. Povacoat[®] (Fig. 2) is a new aqueous polyvinyl alcohol copolymer which has demonstrated potential to effectively prevent the aggregation of nanoparticles of poorly water-soluble compounds. The main advantages of using polymers instead of conventional stabilizers as polysorbates comprise the potential to minimize the molecular motion of the dispersed drug in the solution, prevent the crystal growth and nucleation of the dissolved drug, maintain the supersaturation level for a long period of time, and improve the storage stability by inhibiting the recrystallization of amorphous drug. In addition, povacoat[®] exhibit both hydrophobic and hydrophilic properties, so the surface of a poorly water-soluble compound can be properly wetted and then sterically stabilized in a liquid medium.^{27,28} The low ZP values observed in the povacoat[®] formulations (FB and FC) indicate a sterically stabilized system, what possibly compensate the free energy of the new surfaces created and help to avoid agglomeration, nucleation, and crystal growth; however, the main stabilization mechanisms are still unclear and further investigation is needed to develop better and more rational screening strategies. Additionally, the PDI of FA was increased to 0.452, whereas for FB and FC there were no significant changes in the PDI values. Values higher than 0.500 are related to the Ostwald ripening, being considered critical in the formulation.^{33,34}

ZP analysis is based on the assessment of the movement of the particles in an electric field, being a fundamental parameter in the

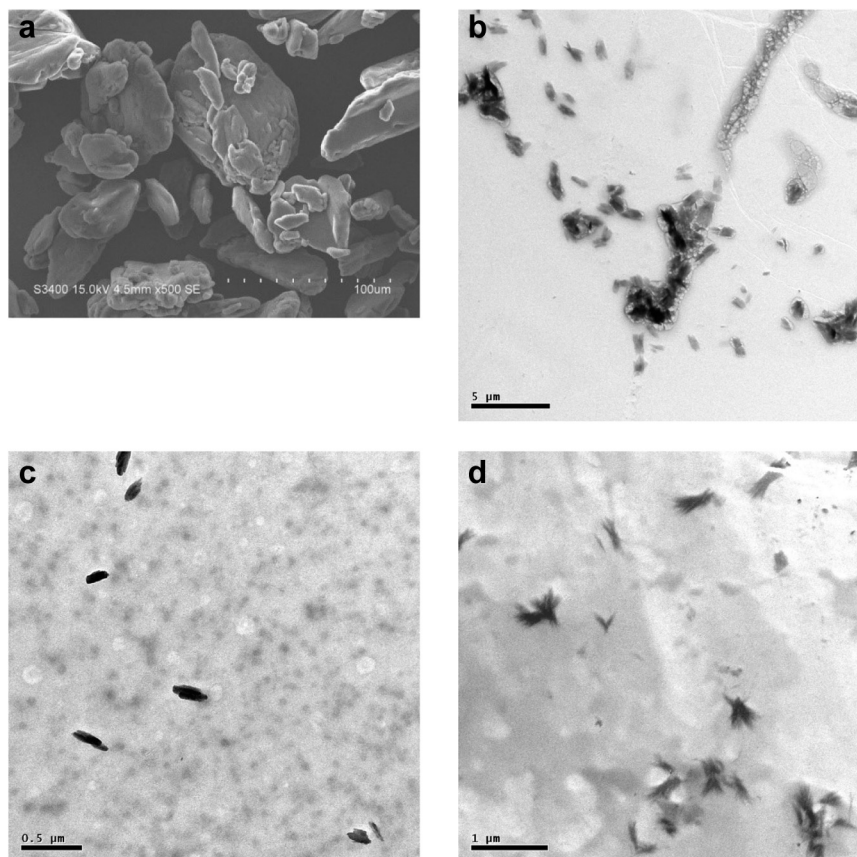


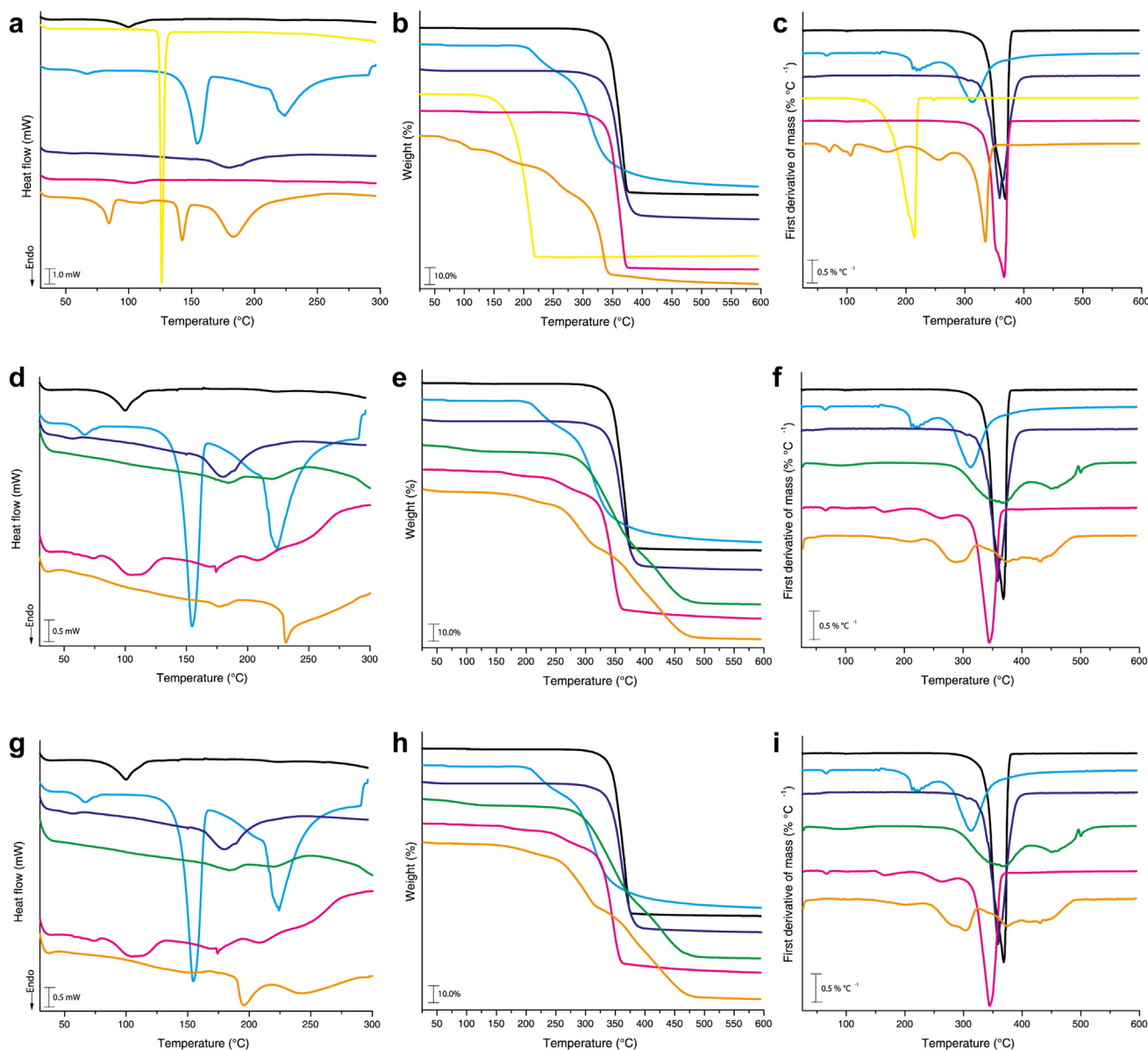
Figure 4. Images of OA raw material (a), FA (b), FB (c), and FC (d).

prediction of long-term stability. At the end of the third month, ZP values were -30.3 ± 8.4 mV, -4.7 ± 7.5 mV, and -9.8 ± 7.2 mV, respectively, for FA, FB, and FC. A ZP of at least -30 mV for electrostatic and -20 mV for sterically stabilized systems is desired to obtain a physically stable nanosuspension.³⁵ However, there is no general rule.³⁶⁻³⁹ ZP values are dependent on the type, size, molecular weight, and other stabilizer characteristics. Müller³⁹ established the ZP value of polysorbate alone (-13 mV) and posteriorly this value in a very sterically stabilized system (-3 mV). The authors observed that ZP values lower than -30 mV and -20 mV can be observed without breakage in the system. By contrast, the use of polysorbate was reported as critical for long-term stability due to its relatively thin adsorbed layer in the nanoparticles.^{38,40} In summary, the feasibility of its use should be monitored case by case. In the present study aiming to provide effective steric stabilization, different classes of stabilizers were used: a nonionic surfactant

(polysorbate 80), a semisynthetic nonionic polymer (methylcellulose), and a polymer (povacoat[®]). Their influence on the stability was statistically evaluated.

Additionally, both formulations were easily redispersed with water during this period. In contrast, FA was challenging to redisperse in water, after lyophilization, possibly due to the irreversible nanocrystal aggregation.

The results from the stability study were evaluated using ANOVA, a parametric method, which is reliable and powerful in detecting differences in quantitative data. In ANOVA, values of a significance level (p values) less than 0.05 ($\alpha = 0.05$) indicate statistically significant models.⁴¹ Thus, ANOVA was used as a statistical tool to evaluate the interaction among storage time, povacoat[®], and polysorbate 80, on z -average, ZP and PDI. For z -average (Fig. 3a), povacoat[®] and storage time presented p values < 0.05 , 0.008, and 0.02, respectively. For ZP (Fig. 3b), povacoat[®], polysorbate 80, and time



Orotic acid – Methylparaben – Glucose – Methylcellulose – Povacoat – Physical mixture – FA/ FB/ FC

Figure 5. Thermoanalytic profiles obtained in dynamic nitrogen atmosphere (50 mL min^{-1}) and heating rate 5°C min^{-1} : (a) DSC, (b) TG, and (c) DTG curves of OA raw material, physical mixture, excipients, and FA. (d) DSC, (e) TG, and (f) DTG curves of OA raw material, physical mixture, excipients, and FB. (g) DSC, (h) TG, and (i) DTG curves of OA raw material, physical mixture, excipients, and FC.

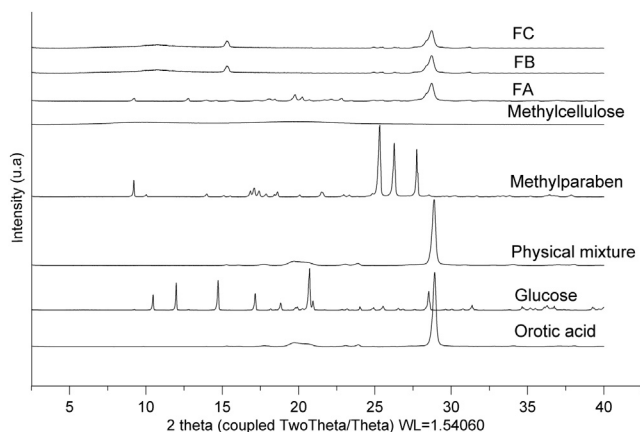


Figure 6. X-ray diffractogram of OA raw material, physical mixture, excipients, and FA, FB, and FC.

presented *p* values of 0.001, 0.440, and 0.066, respectively. For PDI (Fig. 3c), *p* values were 0.012 for povacoat® and time. In summary, these analyses showed that povacoat® and the storage time influenced the stability of the nanocrystals. The analysis also revealed that the total absence of this polymer was the determining factor for increasing the z-average and PDI values. A similar advantage of this polymer was identified by Yuminoki et al.⁴² to stabilize griseofulvin, probucol, tolbutamide, and hydrochlorothiazide nanocrystals by using high-energy milling. The author found povacoat® was the most effective in preventing nanocrystal aggregation compared to hydroxypropyl cellulose and polyvinylpyrrolidone.

SEM Analysis

One of the main advantages of using microscopy techniques in characterizing nanocrystal is to reveal its size independent of the particle shape. Keck⁴³ pointed out a critical shortcoming of these traditional measurement techniques. According to the author, DLS and DL techniques assume sphere-shaped particles for the measurement of the z-average and particle size distribution, respectively. In general, nanocrystals rarely present a sphere shape. Thus, the particle size obtained is estimated, demonstrating the importance of using a supplementary technique to overcome this limitation.⁴⁴

Microscopy images (Fig. 4) revealed differences in size, surface, and shape of OA raw material (Fig. 4a) compared to nanocrystals (Figs. 4b-4d). Additionally, they revealed the presence of clusters of OA raw material (Fig. 4a), which confirms the results obtained previously by DLS and DL (PDI, 0.424). For FA, although PDI was

0.179 ± 0.05 using the DLS technique, microscopy images showed aggregation (Fig. 4b). Moreover, it is possible to observe the effectiveness of the milling process in the reduction of the particle size (Figs. 4b-4d). The Image J software allowed determining the crystal particle size, being 354 ± 45 nm, 141 ± 22 nm, and 116 ± 26 nm, respectively, for FA, FB, and FC ($n = 30$). Due to the diversity in shape and size that nanocrystals can present, software such as Image J are being widely used to certify these parameters, even when the traditional methods (DLS and DL) are used.⁴⁵⁻⁴⁹

OA nanocrystals apparently presented a needle shape for all formulations. Nanocrystal shape is a distinct parameter of each substance and is closely related to the type of vessel, centrifugal force, running time, and specific characteristics of the zirconia balls used during the milling process.²²

Thermal Analysis

Thermal properties of OA raw material and FA, FB, and FC were evaluated by DSC (Figs. 5a, 5d, and 5g, respectively), TG (Figs. 5b, 5e, and 5h), and DTG (Figs. 5c, 5f, and 5i) analysis. TG profile of OA indicates the presence of 2 main events during the mass loss. The first event occurs between 100°C and 150°C and corresponds to the sample dehydration, suggesting that the anhydrous OA probably was converted into a hydrate during transport or storage. According to Braun et al.,⁵⁰ anhydrous OA can transform into the hydrate form during storage time, depending on relative humidity of the environment. Also, a second step assigned to sublimation occurs at 330°C, corresponding to a mass loss of 99.8%, which is followed by a slow final decomposition step.

TG/DTG curve of FA (Figs. 5b and 5c) exhibits the first mass loss between 50°C and 80°C ($\Delta m = 2.6\%$; $T_{\text{peak}} = 70^\circ\text{C}$), which is assigned to dehydration. Posteriorly, 5 additional events with consecutive mass loss ($\Delta m_1 = 5.4\%$, $\Delta m_2 = 9.7\%$, $\Delta m_3 = 17.2\%$, and $\Delta m_4 = 53.8\%$) in the range from 105°C to 335°C ($\text{DTG}_{\text{peak}} = 105^\circ\text{C}$, 169°C , 256°C , and 335°C), followed by a slow final step at 355°C. For FB (Figs. 5e and 5f) and FC (Figs. 5h and 5i), the water loss process is less pronounced and it occurs near 50°C. Posteriorly, 2 additional events of mass loss are observed at 268°C (extrapolated onset temperature = T_{onset}) and 231°C for FB and FC, respectively. Finally, both formulations present a slow final step between 474°C and 482°C.

DSC curves confirmed most of the events observed by TG analysis. DSC curve of FA (Fig. 5a) shows a well-defined endothermic event near to 85°C ($T_{\text{peak}} = 84^\circ\text{C}$), confirming the presence of the OA hydrate. For FB and FC, Figures 5d and 5g, respectively, a broad endothermic event occurs gradually from 25°C, indicating the presence of a small amount of water superficially adsorbed, that is, not bound to the structure. These results clearly indicate structural differences and that the freeze-drying process was not efficient to

Table 1
Saturation Solubility ($N = 3$) of OA Raw Material, Physical Mixtures of FA (PM-FA), FB (PM-FB), and FC (PM-FC), Nanocrystal Formulations (FA, FB, and FC), and the Increase in Solubility

Formulation	Media (mg/mL)						Increase in Solubility (Times)	
	Water		Acetate pH 4.5				Water	Acetate pH 4.5
OA	0.10	0.11	0.10	0.20	0.18	0.19	RV	RV
PM-FA	0.09	0.10	0.09	0.21	0.20	0.20	—	—
PM-FB	0.11	0.11	0.10	0.22	0.21	0.21	—	—
PM-FC	0.11	0.10	0.10	0.19	0.20	0.20	—	—
FA	1.35	1.37	1.36	2.20	2.22	2.20	13.6	11.0
FB	0.65	0.66	0.63	1.50	1.48	1.51	6.3	7.5
FC	0.65	0.56	0.56	1.02	1.03	1.04	5.6	5.0

RV, reference value; —, not observed; OA, orotic acid raw material; PM-FA, physical mixture of orotic acid, methylcellulose, polysorbate 80, and glucose; PM-FB, physical mixture of orotic acid, methylcellulose, polysorbate 80, povacoat®, and glucose; PM-FC, physical mixtures of orotic acid, methylcellulose, povacoat®, and glucose; FA, nanocrystal formulation FA; FB, nanocrystal formulation FB; FC, nanocrystal formulation FC.

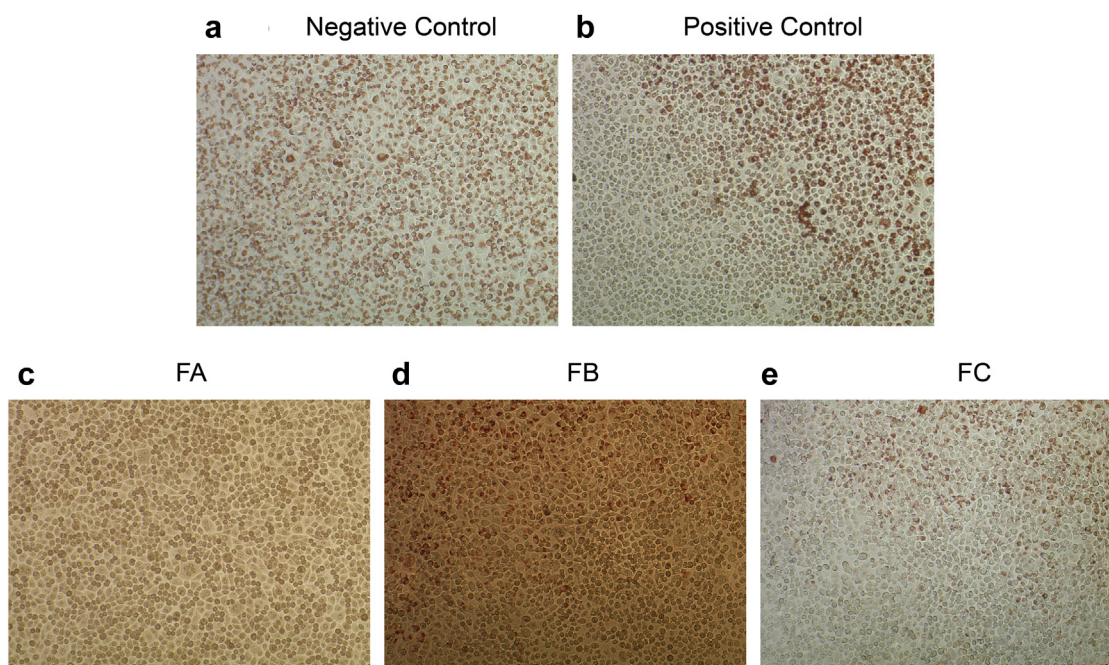


Figure 7. Images of cytotoxicity assay. Negative control (a), positive control (b), FA (c), FB (d), and FC (e).

remove bound water from FA formulation. A second endothermic event in the DSC FA curve corresponds to the anticipation of the melting point of glucose ($T_{\text{peak}} = 143^{\circ}\text{C}$). The third endothermic event is observed at about 183°C ($T_{\text{peak}} = 183^{\circ}\text{C}$), which suggests the anticipation of glucose decomposition. In case of FB/FC, events related to povacoat[®] melting were characterized by endothermic events, occurring from 160°C to 170°C , and by exothermic recrystallization events at 170°C and 190°C .⁵¹ Thereafter, an endothermic event related to the decomposition of glucose is observed near 200°C ($T_{\text{peak}} = 197^{\circ}\text{C}$), followed by povacoat[®] decomposition between 231°C and 237°C (FB $T_{\text{peak}} = 231^{\circ}\text{C}$, FC $T_{\text{peak}} = 237^{\circ}\text{C}$).

X-Ray Diffraction

The X-ray diffraction pattern of OA raw material exhibited reflections of high intensity, narrow and a well-defined boundary, indicating its crystalline nature (Fig. 6). The most intense peak of OA (at 29°) is also preserved in the formulations and physical mixture. Comparing the OA raw material with FA, FB, and FC, we observed that the nanocrystals showed lower intensity in the diffraction patterns. This fact is probably caused by the significant reduction in the particle size induced by the milling process and the addition of certain degree of disorder due to amorphization and/or hydration.⁵⁰ FB and FC patterns have more similarities between them than compared to FA, in agreement with the thermal analysis results.

Determination of Saturation Solubility

Solubility test was performed using the media acetate pH 4.5 and water, which were selected from an exploratory solubility test on OA raw material. In these media, OA presented higher saturation solubility than pH 1.2 and 6.8 and 7.2. As shown in Table 1, FA, using water, revealed the highest increase in the saturation solubility, reaching up to 13 times higher than OA raw material. FB exhibited an increase in saturation solubility up to 7.5 times higher in acetate buffer pH 4.5 compared to OA raw material. For FC, it was demonstrated that the increase in solubility was practically the same in both media: 5 times higher. Barbosa et al.¹⁷ obtained

furosemide nanocrystals, using high-energy milling, with saturation solubility between 1.2 and 3.0 times higher compared to the furosemide raw material.

According to the study of the physical mixtures, no enhancement in saturation solubility was observed compared to values of OA raw material (Table 1). These results confirm that the improvement in saturation solubility of nanocrystals was due to reduction in the particle size revealing innovative physical and chemical characteristics.⁵² Among these nanocrystal particularities, the most known are the increased surface area, the rise in adhesiveness, and dissolution rate of poorly water-soluble drugs. These effects are elucidated by Noyes-Whitney, Kelvin, and Ostwald-Freundlich equations.^{21,44,53,54} In general, these properties lead to improved bioavailability, provide rapid onset of action, reduction in fasted/fed state variations,¹⁴ reduction in volume and dosages administered,^{35,55} and enhanced skin delivery.^{56,57}

Additionally, some studies demonstrated that high-energy milling was the most effective method for preparing oral suspensions for pharmacological, pharmacokinetic, and safety studies on animals during the drug discovery and preclinical phase. Furthermore, it has enough potential to warrant expanding research into a new approach for preparing extemporaneous formulations for the first-in-human and early clinical studies of a candidate drug.²²

Cytotoxicity

The agar diffusion test is a qualitative assessment of toxicity, which is used as a screening evaluation in developing process of new products due to its practicality and low cost. This method proved to be suitable for screening assays and evaluating the toxicity of new products basing themselves on their ability to predict irritation *in vivo*. In addition, it contributes significantly to reducing animal assays.⁵⁸⁻⁶¹ According to US Pharmacopeia,³² the cytotoxicity of FA, FB, and FC was classified by the size of cell death area on the plate. The results can be observed in Figure 7. FA (Fig. 7c) presented cell death in the entire plate and its graded reactivity was grade 4 (severe toxicity). However, both FB (Fig. 7d) and FC (Fig. 7e) showed average cell death area of 0.133 cm and

0.139 cm, respectively, and was graded as grade 2 (mild toxicity). The severe cytotoxicity shown by FA could be explained due to the high concentration of OA in formulation (42.5%). FB and FC showed mild toxicity probably due to the difference of excipients in the formulations; besides, the OA content was more than 3 times lower than in FA. Although the nanocrystals might be used as a primary formulation, this toxicity presented by the FA must be investigated, considering the concentration that will be used in the final product.

Conclusion

High-energy milling technique successfully allowed a particle size reduction of OA to the nanosize range (100-200 nm). The nanocrystals obtained presented a significant increase in the saturation solubility compared to OA raw material, up to 13 times. Povacoat[®], as stabilizer agent, provided stable formulations with improved and better physicochemical characteristics. Additionally, cytotoxicity assay revealed mild toxicity for the stable formulations which could be improved by controlling the final concentration in the formulation. Thus, OA nanocrystals produced with povacoat[®] have the potential, as a platform, to develop unique drug products, cosmetics, and food supplements.

Acknowledgments

CNPq, (The Brazilian National Council for Scientific and Technological Development) and FAPESP (The São Paulo Research Foundation) are the primary funders, Instituto Adolfo Lutz, Think Corporation, Daido Chemical. Jim Hesson of AcademicEnglishSolutions.com revised the English of this article.

References

- Kacso I, Borodi G, Fárcaş SI, Bratu I. Inclusion compound of vitamin B13 in β -cyclodextrin. Structural investigations. *J Phys Conf Ser*. 2009;189:1-4.
- Cuellar A, Alcolea MP, Rastogi VK, Kiefer W, Schlücker S, Rathor SK. FT-IR and FT-Raman spectra of 5-fluorouracil acid with solid state simulation by DFT methods. *Spectrochim Acta A Mol Biomol Spectrosc*. 2014;132:430-445.
- Krungkrai J, Krungkrai SR, Phakanont K. Antimalarial activity of orotate analogs that inhibit dihydroorotase and dihydroorotase dehydrogenase. *Biochem Pharmacol*. 1992;43(6):1295-1301.
- Christopherson RI, Lyons SD, Wilson PK. Inhibitors of de novo nucleotide biosynthesis as drugs. *Acc Chem Res*. 2002;35(11):961-971.
- Jasmin G, Proschek L. Effect of orotic acid and magnesium orotate on the development and progression of the UM-X7.1 hamster hereditary cardiomyopathy. *Cardiovasc Drugs Ther*. 1998;12(Suppl 2):189-195.
- Rosenfeldt FL, Richards SM, Lin Z, Pepe S, Conyers RA. Mechanism of cardioprotective effect of orotic acid. *Cardiovasc Drugs Ther*. 1998;12(Suppl 2):159-170.
- Geiss KR, Stergiou N, Jester, Neuenfeldt HU, Jester HG. Effects of magnesium orotate on exercise tolerance in patients with coronary heart disease. *Cardiovasc Drugs Ther*. 1998;12(Suppl 2):153-156.
- Meerson FZ, Rosanova LS. Effect of actinomycin and combination of nucleic acid synthesis activators on the development of fatigue and fitness. *Dokl Akad Nauk SSSR*. 1967;166:496-499.
- Hasunuma K, Abe T, Masahiro K, Kanebo LTD. Cosmetic composition containing vitamin E orotate. US n° 4000276A, 24 ago. 1973, 28 dez. 1976. Available at: <http://www.freepatentsonline.com/4000276.html>. Accessed April 27, 2014.
- Refat MS, Alghool S, El-Halim HFA. Alkaline earth metal (II) complexes of vitamin B13 with bidentate orotate ligands: synthesis, structural and thermal studies. *CR Chim*. 2010;14(5):496-502.
- Müller RH, Keck CM. Twenty years of drug nanocrystals: where are we, and where do we go? *Eur J Pharm Biopharm*. 2012;80(1):1-3.
- Mauludin R, Muller RH. Physicochemical properties of hesperidin nanocrystal. *Int J Pharm Pharm Sci*. 2013;5:954-960.
- Müller RH, Gohla S, Keck CM. State of the art of nanocrystals: special features, production, nanotoxicology aspects and intracellular delivery. *Eur J Pharm Biopharm*. 2011;78(1):1-9.
- Gao L, Liu G, Ma J, et al. Application of drug nanocrystal technologies on oral drug delivery of poorly soluble drugs. *Pharm Res*. 2013;30(2):307-324.
- Junyaprasert VB, Morakul B. Nanocrystals for enhancement of oral bioavailability of poorly water-soluble drugs. *Asian J Pharm Sci*. 2014;10(1):13-23.
- Chen ML, John M, Lee SL, Tyner KM. Development considerations for nanocrystal drug products. *AAPS J*. 2017;19(3):642.
- Barbosa SF, Takatsuka T, Tavares GD, et al. Physical-chemical properties of furosemide nanocrystals developed using rotation revolution mixer. *Pharm Dev Technol*. 2016;21(7):812-822.
- Jog R, Burgess DJ. Pharmaceutical amorphous nanoparticles. *J Pharm Sci*. 2017;106(1):39-65.
- Möschwitzer JP. Drug nanocrystals in the commercial pharmaceutical development process. *Int J Pharm*. 2013;453(1):142-156.
- Xia D, Gan Y, Cui F. Application of precipitation methods for the production of water-insoluble drug nanocrystals: production techniques and stability of nanocrystals. *Curr Pharm Des*. 2014;20(3):408-435.
- Sinha B, Müller RH, Möschwitzer JP. Bottom-up approaches for preparing drug nanocrystals: formulations and factors affecting particle size. *Int J Pharm*. 2013;453(1):126-141.
- Takatsuka T, Endo T, Jianguo Y, Yuminoki K, Hashimoto N. Nanosizing of poorly water soluble compounds using rotation revolution mixer. *Chem Pharm Bull*. 2009;57(10):1061-1067.
- Chen H, Chalermchai K, Xiangliang Y, Xueling C, Jinming G. Nanonization strategies for poorly water-soluble drugs. *Drug Discov Today*. 2011;16(7-8):354-360.
- THINKY CORPORATION (Org.). Wet pulverizing. Available at: <http://www.thinkyusa.com/commentary/funsai.html>. Accessed May 20, 2010.
- Peltonen L, Hirvonen J. Pharmaceutical nanocrystals by nanomilling: critical process parameters, particle fracturing and stabilization methods. *J Pharm Pharmacol*. 2010;62:1569-1579.
- Eerdenbrugh B, Mooter G, Augustijns P. Top-down production of drug nanocrystals: nanosuspension stabilization, miniaturization and transformation into solid products. *Int J Pharm*. 2008;364(1):64-75.
- Yuminoki K, Seko F, Horii S, et al. Application of povacoat as dispersion stabilizer of nanocrystal formulation. *Asian J Pharm Sci*. 2016;11(1):48-49.
- Yuminoki K, Seko F, Horii S, et al. Preparation and evaluation of high dispersion stable nanocrystal formulation of poorly water-soluble compounds by using povacoat. *J Pharm Sci*. 2014;103(11):3772-3781.
- Romero GB, Keck CM, Müller RH, Bou-Chacra NA. Development of cationic nanocrystals for ocular delivery. *Eur J Pharm Biopharm*. 2016;107:215-222.
- United States Pharmacopeia and National Formulary (USP 33-NF 28). 4. Rockville, MD: United States Pharmacopeial Convention; 2010.
- International Organization for Standardization. ISO 10993-5: Biological Evaluation of Medical Devices. Part 5. Test of Cytotoxicity: In Vitro Methods. Geneva: ISO; 2009:9.
- United States Pharmacopeia and National Formulary [USP 39 NF 34]. 3. Rockville, MD: United States Pharmacopeial Convention; 2015.
- Rabinow BE. Nanosuspensions in drug delivery. *Nat Rev Drug Discov*. 2004;3(9):785-796.
- Verma S, Lan Y, Gokhale R, Burgess DJ. Quality by design approach to understand the process of nanosuspension preparation. *Int J Pharm*. 2009;371:185-198.
- Gao L, Zhang D, Chen M. Drug nanocrystals for the formulation of poorly soluble drugs and its application as a potential drug delivery system. *J Nanopart Res*. 2008;10(5):845.
- Muller RH, Peters K. Nanosuspensions for the formulation of poorly soluble drugs. Preparation by a size-reduction technique. *Int J Pharm*. 1998;160(2):229-237.
- Tuomela A, Hirvonen J, Peltonen L. Stabilizing agents for drug nanocrystals: effect on bioavailability. *Pharmaceutics*. 2016;8(2):16-34.
- Riddick TM. *Control of Colloid Stability Through Zeta Potential*. 1st ed. Wynnewood, PA: Livingston Publishing Company; 1968.
- Müller Rainer H. *Colloidal Carriers for Controlled Drug Delivery and Targeting: Modification, Characterization and in Vivo Distribution*. 1st ed. Stuttgart: Taylor & Francis; 1991:379.
- Mishra PR, Al Shaal L, Müller RH, Keck CM. Production and characterization of Hesperetin nanosuspensions for dermal delivery. *Int J Pharm*. 2009;371(1-2):182-189.
- Myers RH, Montgomery DC, Anderson-cook CM. *Response Surface Methodology: Process and Product Optimization Using Designed Experiments*. 3rd ed. Hoboken: John Wiley; 2009:704.
- Yuminoki K, Takeda M, Kitamura K, et al. Nano-pulverization of poorly watersoluble compounds with low melting points by a rotation revolution pulverizer. *Pharmazie*. 2012;67(8):681-686.
- Keck CM. Particle size analysis of nanocrystals: improved analysis method. *Int J Pharm*. 2009;390(1):3-12.
- Keck CM, Müller RH. Size analysis of submicron particles by laser diffractometry—90% of the published measurements are false. *Int J Pharm*. 2007;355(1-2):150-163.
- Choi JS, Park JS. Development of docetaxel nanocrystals surface modified with transferrin for tumor targeting. *Drug Des Devel Ther*. 2016;11:17-26.
- Chen F, Huang P, Zhu YJ, Wu J, Zhang CL, Cui DX. The photoluminescence, drug delivery and imaging properties of multifunctional Eu³⁺/Gd³⁺ dual-doped hydroxyapatite nanorods. *Biomaterials*. 2011;32(34):9031-9039.
- Teodoro JS, Simões AM, Duarte FV, et al. Assessment of the toxicity of silver nanoparticles in vitro: a mitochondrial perspective. *Toxicol In Vitro*. 2011;25(3):664-670.
- Ma M, Huang Y, Chen H, et al. Bi2S3-embedded mesoporous silica nanoparticles for efficient drug delivery and interstitial radiotherapy sensitization. *Biomaterials*. 2015;37:447-455.
- Sohn JS, Yoon DS, Sohn JY, Park JS, Choi JS. Development and evaluation of targeting ligands surface modified paclitaxel nanocrystals. *Mater Sci Eng C Mater Biol Appl*. 2017;72:228-237.

50. Braun DE, Nartowski KP, Khimyak YZ, Morris KR, Byrn SR, Griesser UJ. Structural properties, order–disorder phenomena, and phase stability of orotic acid crystal forms. *Mol Pharm.* 2016;13(3):1012-1029.
51. Xu M, Zhang C, Luo Y, et al. Application and functional characterization of POVACOAT, a hydrophilic co-polymer poly(vinyl alcohol/acrylic acid/methyl methacrylate) as a hot-melt extrusion carrier. *Drug Dev Ind Pharm.* 2014;40(1):126-135.
52. Mauludin R, Muller RH, Keck CM. Development of an oral rutin nanocrystal formulation. *Int J Pharm.* 2009;370(1-2):202-209.
53. Noyes AA, Whitney WR. The rate of solution of solid substances in their own solutions. *J Am Chem Soc.* 1897;19(12):930-934.
54. Buckton G, Beezer AE. The relationship between particle size and solubility. *Int J Pharm.* 1992;82(3):7-10.
55. Rabinow B, Kipp J, Papadopoulos P, et al. Itraconazole IV nanosuspension enhances efficacy through altered pharmacokinetics in the rat. *Int J Pharm.* 2007;339(1-2):251-260.
56. Shegokar R, Muller R. Nanocrystals: industrially feasible multifunctional formulation technology for poorly soluble actives. *Int J Pharm.* 2010;399(1-2):129-139.
57. Vidlářová L, Romero GB, Hanuš J, Stěpánek F, Müller RH. Nanocrystals for dermal penetration enhancement – effect of concentration and underlying mechanisms using curcumin as model. *Eur J Pharm Biopharm.* 2016;104:216-225.
58. Pinto TJA, Ikeda TI, Miyamaru LL, Bárbara MCS, Santos RP, Cruz AS. Cosmetic safety: proposal for the replacement of in vivo (Draize) by in vitro test. *Open Toxicol J.* 2009;3:1-7.
59. Wood N, Ferguson JL, Gunaratne HQN, Seddon KR, Royston G, Stephens GM. Screening ionic liquids for use in biotransformations with whole microbial cells. *Green Chem.* 2011;13(7):1843-1851.
60. Bauer AW, Kirby WM, Sherris JC, Turck M. Antibiotic susceptibility testing by a standardized single disk method. *Am J Clin Pathol.* 1996;45(4):493-496.
61. Vedel G, Peyret M, Gayral JP, Millot P. Evaluation of an expert system linked to a rapid antibiotic susceptibility testing system for the detection of beta-lactam resistance phenotypes. *Res Microbiol.* 1996;147(4):297-309.